Optical Zeeman effect measurements on isolated and ferromagnetically coupled Nd^{3+} ions in weakly doped YVO_4 crystals: evidence for lack of crystal field perturbations in ion pair interactions

2000 J. Phys.: Condens. Matter 12 7149

(http://iopscience.iop.org/0953-8984/12/31/315)

J. Phys.: Condens. Matter **12** (2000) 7149–7160. Printed in the UK PII: S0953-8984(00)13990-6

Optical Zeeman effect measurements on isolated and ferromagnetically coupled Nd^{3+} ions in weakly doped YVO_4 crystals: evidence for lack of crystal field perturbations in ion pair interactions

V Mehta†§, O Guillot-Noël†, D Gourier†‖, Z Ichalalène‡, M Castonguay‡ and S Jandl‡

† Ecole Nationale Supérieure de Chimie de Paris (ENSCP), Laboratoire de Chimie Appliquée de l'Etat Solide, UMR CNRS 7574, 11 rue Pierre et Marie Curie, 75231 Paris Cédex 05, France
‡ Centre de recherche en Physique du Solide, Département de Physique, Université de Sherbrooke, Sherbrooke, Québec, Canada J1K2R1

E-mail: gourierd@ext.jussieu.fr (D Gourier)

Received 18 May 2000

Abstract. Optical Zeeman effect measurements are performed at liquid helium temperature on Nd^{3+} ions in weakly doped YVO_4 crystals in the range 11 350–11 390 cm^{-1} of the $^4F_{3/2} \rightarrow {}^4I_{9/2}$ neodymium transitions. This study provides confirmation that the concentration dependent satellite lines accompanying the optical transitions are due to ferromagnetically coupled pairs of Nd^{3+} ions in undistorted Y^{3+} sites of D_{2d} point site symmetry. Nonlinear Zeeman splittings are observed in the range of experimental magnetic fields. These splittings are compared with those simulated from crystal field calculations by introducing the Zeeman Hamiltonian into the secular determinant before diagonalization. A reasonably good agreement between the calculated and experimental g-values is obtained, confirming that the exchange coupled neodymium pairs experience no crystal field perturbations.

1. Introduction

The existence of satellite lines in the optical spectra of rare earth ions in condensed matter, even at low doping levels, is a well known problem which has given rise to many studies [1–9]. The interpretations concerning their origin are not always consistent. These extra lines could be due to rare earth ions occupying distinct sites in a crystal, each site giving rise to its own spectrum. The distinctions can arise from inequivalent sites [4] and/or distortions of similar sites either by neighbouring lattice defects [5] or by neighbouring perturbing ions [3]. Besides, an important cause of satellites could be the interactions between rare earth ion pairs or clusters [4–9]. For instance, these pair interactions are responsible for the appearance of many additional lines in the optical spectra of trivalent neodymium ion in principal laser crystals like yttrium lithium fluoride ($LiYF_4$) [6], yttrium orthovanadate (YVO_4) [8], yttrium aluminium perovskite ($YAlO_3$) [9] and yttrium aluminate garnet ($Y_3Al_5O_{12}$, YAG) [4]. Moreover, Hehlen and co-workers have recently shown that pairs of rare earth ions (Yb^{3+}) exhibit an intrinsically

§ On leave from Kalindi College, University of Delhi, East Patel Nagar, New Delhi 110008, India.
‖ Corresponding author.

0953-8984/00/317149+12$30.00

bistable luminescence resulting from a co-operative effect due to ion–ion coupling within the dimer [10]. Energy migration between pairs has a degrading effect and only isolated ion-pair centres in a weakly doped matrix may exhibit bistability. Thus, a deeper understanding of ion–ion coupling mechanisms in such pairs is of fundamental interest, and could help to optimize the bistable luminescence effect.

Different experimental methods can be used to study the coupling mechanisms in pair or cluster centres. Electron paramagnetic resonance (EPR) is an efficient spectroscopy to study ground state splitting and spin–spin interaction of a coupled system while absorption, fluorescence and excitation spectroscopies are useful for investigation of both the ground and excited state pair interactions.

Recently, we have reported EPR and high resolution fluorescence studies on Nd^{3+} ions in weakly doped YVO_4 crystals [8]. The crystal structure belongs to the $I4_1/amd$ space group and Nd^{3+} ions replace yttrium ions in tetragonal sites of D_{2d} point symmetry. In EPR spectra, pairs of satellite lines observed on each side of the main EPR line of isolated Nd^{3+} ions were assigned to Nd^{3+}–Nd^{3+} pairs coupled by magnetic dipolar interaction. As these extra lines were found to be symmetrically placed around the central EPR line of isolated ions, it was inferred that each ion of a pair has the same ground state g-parameters, and thus appears to be at the same Y^{3+} site of D_{2d} symmetry, as isolated ions. These EPR studies, thus, gave the first indication that Nd^{3+} ion pairs are not affected by crystal field effects. High resolution fluorescence studies of $^4F_{3/2} \rightarrow {}^4I_{9/2}$ transitions provided evidence for the existence of ground state ferromagnetic exchange interactions between two ions of a coupled pair [8]. The structure of the concentration dependent optical satellite lines was satisfactorily explained as being due to four different exchange coupled Nd^{3+} ion pairs, characterized by ground state J ferromagnetic interactions in the range +0.8 to +4.9 cm^{-1}. Both ions of the pair were found to be located at regular unperturbed Y^{3+} sites of the YVO_4 matrix. Small mutual crystal field perturbations ($\sim$1 cm^{-1}) of one ion of a pair by its partner were observed only for the pair with high J value.

Recent time resolved site selective excitation and emission studies by Ermeneux and co-workers on Nd:YVO_4 crystals grown by different techniques, and/or having different origins, are also worth mentioning [5]. Reproducible typical site structure observed in infrared excitation and emission spectra was assigned to Nd^{3+} ions in regular unperturbed and perturbed sites of D_{2d} symmetry and also to Nd^{3+} ions in two other kinds of site. However, these authors did not interpret the perturbed sites in terms of Nd^{3+} pairs.

As a continuation of our investigations on the multisite character of neodymium in the YVO_4 matrix, we present in this paper the measurements and simulation of the optical Zeeman effect in the fluorescence spectra. Low temperature Zeeman splittings of the $^4F_{3/2} \rightarrow {}^4I_{9/2}$ transition of isolated and paired Nd^{3+} ions in external magnetic fields up to 6 T, oriented both parallel and perpendicular to the crystallographic c axis, are measured. The magnitude of the Zeeman splitting depends on the g-factors of the electronic levels connected by the optical transition. The g-factors, being crystal field dependent, are quite different for rare earth ions in different sites [11, 12]. Thus, the satellite lines due to ions in different sites should split differently under an external magnetic field. A study of the optical Zeeman effect could, therefore, permit us to decide whether or not the Nd^{3+} ions forming pairs are located at the same undistorted Y^{3+} sites as the isolated ions.

Non-symmetric Zeeman splittings of the fluorescence lines are observed in the range of experimental magnetic fields (i.e. up to 6 T). These are compared with those calculated from crystal field simulations with D_{2d} symmetry by introducing the appropriate Zeeman Hamiltonian into the total secular determinant before diagonalization.

2. Experiment

YVO_4 single crystals with 0.58% neodymium concentration were grown by the Czochralski method. Low temperature (10 K) fluorescence measurements were performed using a 514.5 nm Ar ion laser with a double monochromator and conventional photon counting system. Samples were placed in a 9 T superconducting magnet for light polarized both parallel and perpendicular to the crystallographic c-axis. Spectra with 0.25 cm^{-1} resolution were recorded in the 11 350–11 390 cm^{-1} range of the $^4F_{3/2} \rightarrow {}^4I_{9/2}$ neodymium transitions with the laser power around 50 mW focused on a 100 μm diameter of the sample. The photoluminescence lines were observed in fresh cut surfaces and with multiple different spots in order to insure that no spurious bands, due to impurities or surface defects, affect the measurements.

3. Theoretical background

In a crystal field of D_{2d} symmetry, a particular $^{2S+1}L_J$ state of Nd^{3+} ions is split into $(J + 1/2)$ Kramer doublets (KDs) (labelled as 1, 2, ...). The twofold degeneracy of a KD can only be lifted by an external magnetic field (Zeeman effect). An effective spin $S = \frac{1}{2}$ can, thus, be attributed to each KD. Taking into account the first order Zeeman splitting (normal Zeeman effect), a single optical transition between a ground KD and an excited KD with g-factors g_0 and g_1 respectively, at energy Δ, will split into two transitions at energies $\Delta \pm \beta B[g_0(\theta) - g_1(\theta)]/2$, owing to the selection rules for electric dipole transitions $\Delta S = 0$, $\Delta M_S = 0$. The signs + and − correspond to the components $M_S = \pm\frac{1}{2}$ of the $S = \frac{1}{2}$ effective spin, θ is the angle between the direction of the applied magnetic field B and the symmetry axis of the Y^{3+} site and β is the Bohr magneton. This is the case when the magnetic field splitting is small in comparison with the crystal field splitting. For larger magnetic fields and in cases where different KDs are close in energy, an additional shift quadratic in the magnetic field can appear [13]. To simulate the Zeeman splitting using crystal field calculations, it is then necessary to include the Zeeman operator in the secular determinant before diagonalization [14, 15]. This procedure is used in the present work since the Zeeman effect treated up to first order in perturbation could not explain the non-symmetric magnetic splittings observed experimentally.

The general Hamiltonian of an ion in the presence of crystal and magnetic fields can be written as follows:

$$H = H_{FI} + H_{CF} + H_{ZE} \tag{1}$$

where H_{FI} is the free ion Hamiltonian, H_{CF} the crystal field Hamiltonian and H_{ZE} the Zeeman Hamiltonian.

According to the formalism of Carnall and co-workers [16], H_{FI} is written as

$$H_{FI} = H_0 + \sum_{k=0}^{k=3} E^k(\mathrm{nf}, \mathrm{nf})e_k + \zeta_{4f}A_{SO} + \alpha L(L+1) + \beta G(G_2) + \gamma G(R_7) + \sum_{\lambda=2,\lambda\neq5}^{\lambda=8} T^\lambda t_\lambda \tag{2}$$

where H_0 is the spherically symmetric part, E^k are the Racah parameters and e_k is the angular part of the electrostatic repulsion, ζ_{4f} is the spin–orbit coupling constant and A_{SO} represents its angular part. Parameters α, β and γ are associated with the two-body interactions and Judd parameters T^λ with the three-body interactions. L is the total angular momentum, and $G(G_2)$ and $G(R_7)$ are the Casimir operators.

Following Wybourne's formalism [17], the crystal field Hamiltonian H_{CF} is expressed as

$$H_{CF} = \sum_{k=2}^{4,6}\sum_{q=0}^{k}[B_q^k(C_q^k + (-1)^q C_{-q}^k) + \mathrm{i}S_q^k(C_q^k - (-1)^q C_{-q}^k)] \tag{3}$$

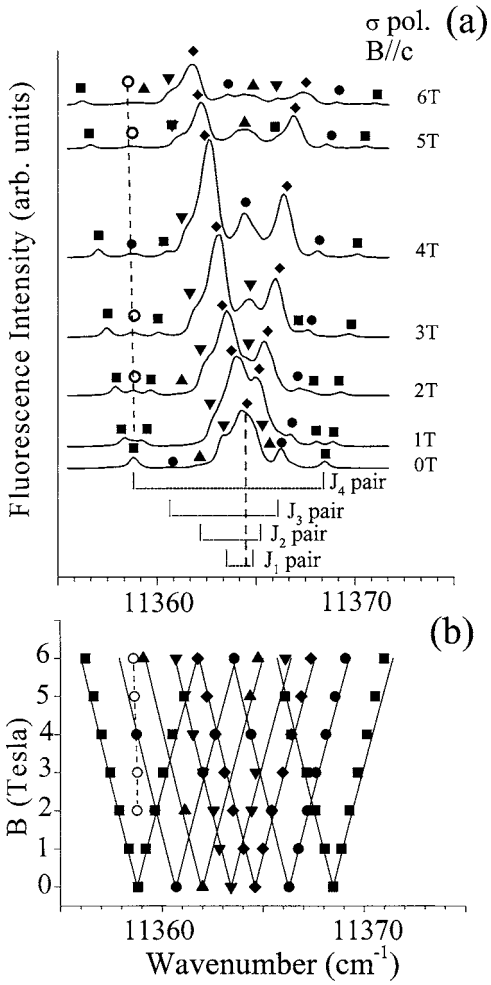

Figure 1. (a) σ-polarized neodymium $^4F_{3/2}(1) \rightarrow {}^4I_{9/2}(1)$ fluorescence spectra at 10 K, with an external magnetic field $B \parallel c$, in the range 0 to 6 T. The main transition (♦) is due to isolated Nd^{3+} ions and the satellite lines indicated by ▼, ▲, ● and ■ are assigned to four types of ferromagnetically coupled pairs of Nd^{3+} ions J_1, J_2, J_3 and J_4, respectively [8]. The vertical discontinuous line in the stick diagram indicates the transition for isolated Nd^{3+} ions. (b) Experimental Zeeman splittings and crystal field simulations (solid curves) calculated for undistorted Nd^{3+} sites with D_{2d} symmetry.

where B_q^k and S_q^k are the real and imaginary parts, respectively, of the crystal-field parameters and C_q^k are Racah operators associated with the spherical harmonics. The number of non-zero crystal field parameters depends on the point site symmetry of the lanthanide ion in the structure. For Nd:YVO_4, the D_{2d} crystal-field Hamiltonian involves five non-zero real B_q^k crystal-field parameters, namely B_0^2, B_0^4, B_4^4, B_0^6 and B_4^6.

The crystal field simulation of the energy level scheme on 96 experimental levels of Nd^{3+} ions in YVO_4 have already been reported by the present authors [18]. We used software programs for simulations of the f^N configuration, involving real and complex crystal field parameters [19]. The free ion and crystal field parameters were calculated without any external magnetic field.

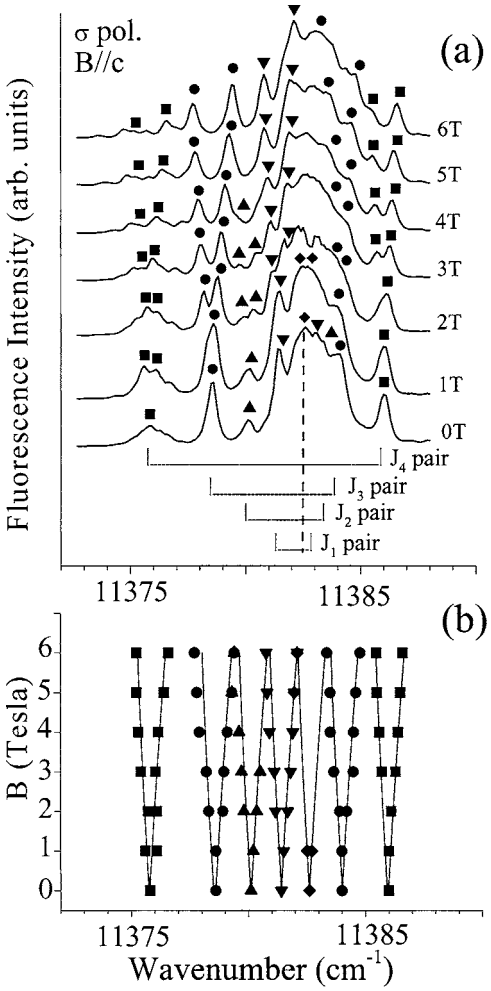

Figure 2. (a) σ-polarized neodymium $^4F_{3/2}(2) \rightarrow {}^4I_{9/2}(1)$ fluorescence spectra at 10 K, with an external magnetic field $B \parallel c$, in the range 0 to 6 T. The symbols have the same meaning as in figure 1. (b) Experimental Zeeman splittings and crystal field simulations (solid curves) calculated for undistorted Nd^{3+} sites with D_{2d} symmetry.

In the presence of the magnetic field, the last term H_{ZE} in equation (1) is introduced into the secular determinant before diagonalization. It is expressed as:

$$H_{ZE} = \beta B(L + g_e S) \tag{4}$$

where β is the Bohr magnetron, S the total spin operator and g_e the free spin g-factor. Previously computed free ion and crystal field parameters are kept constant and B is varied from 0 to 15 T.

4. Results and discussion

The free Nd^{3+} ion has a $4f^3$ configuration. The ground state is $^4I_{9/2}$ and the $^4F_{3/2}$ excited state in YVO_4 is around 11 370 cm^{-1}. The crystal field of D_{2d} point symmetry splits the $^4I_{9/2}$ and the $^4F_{3/2}$ levels into five and two KDs (labelled as 1, 2, ...) at energies 0, 110, 173, 228, 437 cm^{-1} and 11 365, 11 383 cm^{-1}, respectively [18].

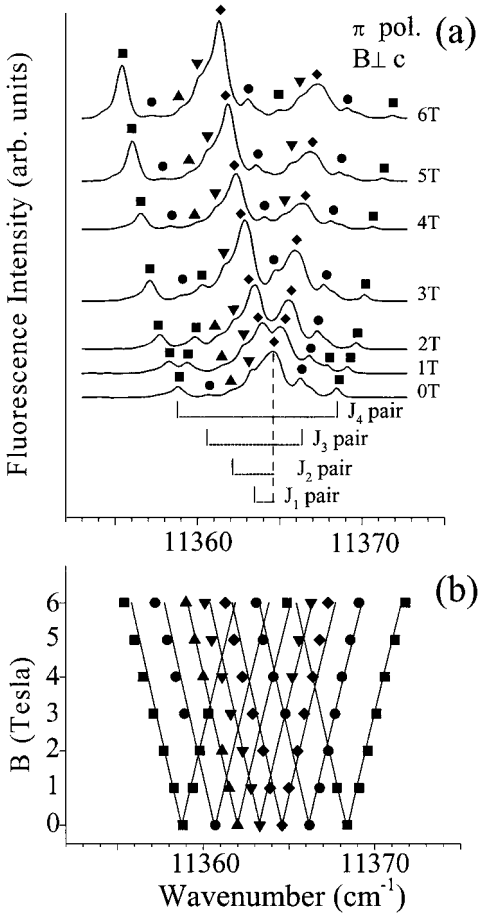

Figure 3. (a) π-polarized neodymium $^4F_{3/2}(1) \rightarrow {}^4I_{9/2}(1)$ fluorescence spectra at 10 K, with an external magnetic field $B \perp c$, in the range 0 to 6 T. The symbols have the same meaning as in figure 1. (b) Experimental Zeeman splittings and crystal field simulations (solid curves) calculated for undistorted Nd^{3+} sites with D_{2d} symmetry.

Figures 1(a) and 2(a) show the σ-polarized $^4F_{3/2}(1) \rightarrow {}^4I_{9/2}(1)$ and $^4F_{3/2}(2) \rightarrow {}^4I_{9/2}(1)$ fluorescence spectra, respectively, for the Nd:YVO_4 (0.58%) sample without and with an external magnetic field B in the range 1 to 6 T, oriented parallel to the crystallographic c-axis. Similar π-polarized emission spectra recorded in the vicinity of $^4F_{3/2}(1) \rightarrow {}^4I_{9/2}(1)$ and $^4F_{3/2}(2) \rightarrow {}^4I_{9/2}(1)$ transitions, with $B \perp c$, are presented in figures 3(a) and 4(a) respectively. As shown in a recent paper [8], the positions of all the main satellite lines around the parent transition (indicated by a diamond shaped symbol in figures 1 to 4), in zero magnetic field, can be satisfactorily explained by assigning them to four different ferromagnetically coupled pairs of Nd^{3+} ions characterized by J coupling values of $J_1 = +0.8(6)\ cm^{-1}$, $J_2 = +1.6(4)\ cm^{-1}$, $J_3 = +2.7(5)\ cm^{-1}$ and $J_4 = +4.9\ cm^{-1}$. For a ground state exchange coupled pair, a doublet of lines is expected at energies $\Delta + J/2$ and $\Delta - 3J/2$, disymmetrically placed around the isolated ion transition at energy Δ [8]. The satellite lines corresponding to the four pairs are indicated by different symbols in figures 1 to 4.

Under an external magnetic field, each line of the spectra splits into two components. Figures 1(b) to 4(b) give a plot of the experimental Zeeman splitting versus magnetic field B

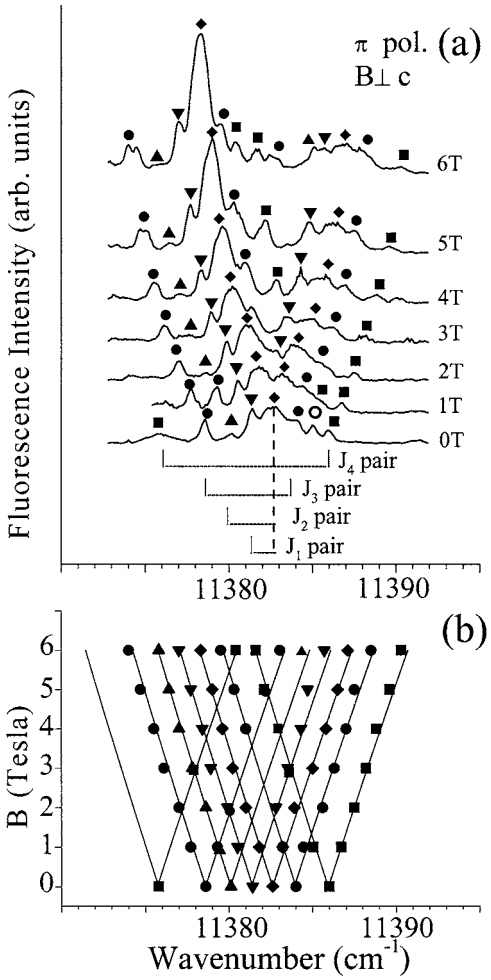

Figure 4. (a) π-polarized neodymium $^4F_{3/2}(2) \rightarrow {}^4I_{9/2}(1)$ fluorescence spectra at 10 K, with an external magnetic field $B \perp c$, in the range 0 to 6 T. The symbols have the same meaning as in figure 1. (b) Experimental Zeeman splittings and crystal field simulations (solid curves) calculated for undistorted Nd^{3+} sites with D_{2d} symmetry.

and for comparison, those obtained from crystal field calculations (shown by solid curves). In all these figures, the positive and negative magnetic shifts of each transition toward increasing and decreasing wavenumbers, respectively, are found to be slightly different from one another. These non-symmetric experimental splittings are in good agreement with crystal field simulations obtained using D_{2d} symmetry and energy levels of isolated Nd^{3+} ions [18]. Moreover, the Zeeman splittings of all the satellite lines are close to one another and to those of the parent line. It can thus be concluded that these extra optical lines are characterized by the same g-values of the KDs under study and consequently, each ion of a pair is located at the regular unperturbed Y^{3+} site of the zircon structure, as the isolated Nd^{3+} ions. Alternately, Nd^{3+} ions located in a different site symmetry should exhibit a different Zeeman splitting. This is the case for the transition indicated by open circles in figure 1. The line hardly shows any magnetic field splitting within the limit of resolution of our optical spectra. Thus this

Table 1. Experimental and crystal field calculated linear Zeeman splittings of the $^4F_{3/2} \rightarrow {}^4I_{9/2}$ transition of isolated Nd^3 ions in YVO_4.

$^4F_{3/2} \rightarrow {}^4I_{9/2}$ transition of isolated Nd^{3+} ions (cm^{-1})	Polarization	Linear Zeeman splitting, $[g_0(\theta) - g_1(\theta)\beta]$	
		Experimental (cm^{-1})	Calculated (cm^{-1})
11 364.6	π	1.02 ± 0.02	1.00
	σ	0.96 ± 0.02	0.96
11 382.6	π	1.49 ± 0.02	1.52
	σ	0.20 ± 0.04	0.20

Table 2. g-factor parameters of the ground state $^4I_{9/2}$ KD and the two $^4F_{3/2}$ KDs of Nd^{3+} in YVO_4.

KD	g-parameters	
	Experimental	Calculated
$^4I_{9/2}(1)$	$\lvert g_0^{\perp}\rvert = 2.361 \pm 0.003$ [20]	$\lvert g_0^{\perp}\rvert = 2.46$
	$\lvert g_0^{\parallel}\rvert = 0.915 \pm 0.004$	$\lvert g_0^{\parallel}\rvert = 0.94$
$^4F_{3/2}(1)$	$\lvert g_1^{\perp}\rvert = 0.18 \pm 0.04$	$\lvert g_1^{\perp}\rvert = 0.34$
	$\lvert g_1^{\parallel}\rvert = 1.13 \pm 0.04$	$\lvert g_1^{\parallel}\rvert = 1.11$
$^4F_{3/2}(2)$	$\lvert g_1^{\perp}\rvert = 0.84 \pm 0.04$	$\lvert g_1^{\perp}\rvert = 0.79$
	$\lvert g_1^{\parallel}\rvert = 0.49 \pm 0.09$	$\lvert g_1^{\parallel}\rvert = 0.51$

fluorescent line could be due to neodymium ions in sites of different point symmetry. By site selective laser excitation and emission experiments performed at low temperature on Nd:YVO_4 crystals, Ermeneux and co-workers have shown the existence of three types of neodymium site, one of them being largely dominant (labelled as site 1) while the other two (sites 2 and 3) are at least one or two orders of magnitude less occupied [5]. An extra optical line in zero magnetic field appearing at the same energy as the one indicated by open circles in figure 1, has been assigned to Nd^{3+} ions in site 2 by these authors. This study confirms why this line behaves so differently in a magnetic field compared to all the other lines (satellite and main lines), attributed to ions in site 1. Another transition indicated by an open circle in figure 4(a) is attributed to Nd^{3+} ions in distorted site 2 [5]. However, this line could not be followed under the external magnetic field.

Figure 5 shows the experimental Zeeman splittings (solid diamonds) of the fluorescent emissions from the two $^4F_{3/2}$ KDs of isolated Nd^{3+} ions in unperturbed sites, in external magnetic fields up to 6 T, along with crystal field simulated magnetic shifts up to 15 T (solid curves). As the magnetic displacement of the $^4F_{3/2}(2) \rightarrow {}^4I_{9/2}(1)$ transition due to isolated Nd^{3+} ions could not be followed experimentally beyond 1 T for $B \parallel c$ (see figure 2), the observed Zeeman pattern (solid squares) of one of the satellite lines accompanying this transition, assigned to J_4 pair, is also shown in figure 5(b). It can be observed from this figure that the splittings of the transitions are non-symmetrical and nonlinear for magnetic fields oriented both perpendicular and parallel to the c-axis. This nonlinear behaviour is due to a quadratic Zeeman effect resulting from a mixing of different KDs close in energy. A simple calculation up to second order in perturbation gives a magnetic dependency of the electronic

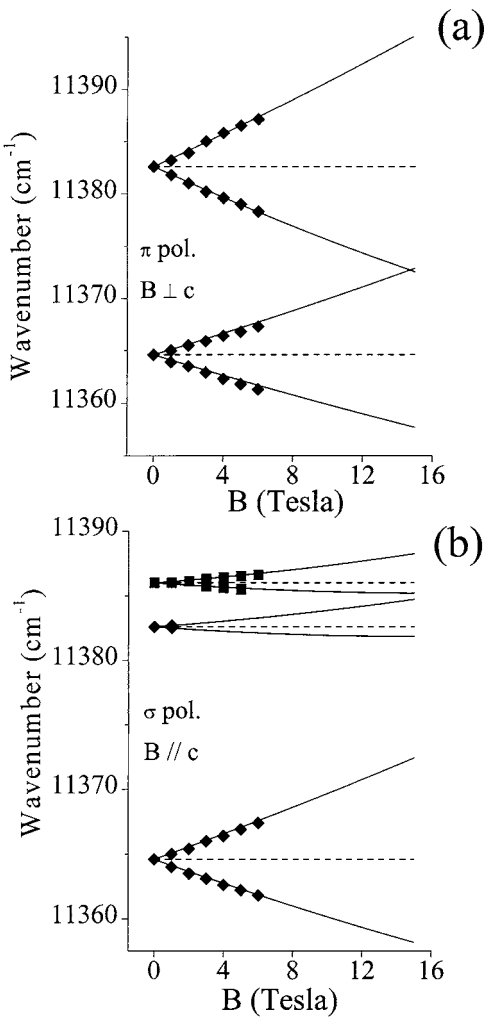

Figure 5. Experimental Zeeman splittings (♦) and crystal field simulations (solid curves) of the Zeeman effect, for the undistorted Nd^{3+} site with D_{2d} symmetry, on the two fluorescence $^4F_{3/2}(1 \text{ and } 2) \rightarrow {}^4I_{9/2}(1)$ neodymium transitions in Nd:YVO_4. (a) π-polarized spectra with $B \perp c$ and (b) σ-polarized spectra with $B \parallel c$; this figure also represents the Zeeman splittings for one transition of the J_4 pair (■). For each line, the non-symmetrical splitting indicates a quadratic Zeeman effect.

energy $E_i(B)$ of an $|i\rangle$ KD of the form:

$$E_i(B) = E_i(0) \pm \beta B \frac{g_i(\theta)}{2} + \sum_f \frac{|\langle f|H_{ZE}|i\rangle|^2}{E_i(0) - E_f(0)} \tag{5}$$

where $|f\rangle$ are all the KDs which mix with the $|i\rangle$ KD via the Zeeman Hamiltonian. The crystal field simulated curves exhibit quadratic magnetic shifts of the order of 10^{-3} cm^{-1} in addition to linear splitting listed in table 1. This leads to a $E_i(0) - E_f(0)$ energy difference of the order of 100 cm^{-1}. As the other KDs of the $^4I_{9/2}$ multiplet are only 110, 173, 228 and 437 cm^{-1} above the fundamental KD, they give the main contribution to the B^2 dependency of the magnetic splitting. In the case of the $^4F_{3/2}$ multiplet, the Zeeman Hamiltonian gives non-zero second order term only when the magnetic field is perpendicular to the c-axis. Indeed, as the two $^4F_{3/2}$ KDs are purely $|\frac{3}{2}, \pm\frac{3}{2}\rangle$ and $|\frac{3}{2}, \pm\frac{1}{2}\rangle$ in the $|J, \pm M_J\rangle$ basis set, only the x and y components S_x and S_y of the effective spin can mix these two KDs and lead to non-zero $\langle f|H_{ZE}|i\rangle$ matrix elements.

The present optical Zeeman effect measurements, combined with our previous ground state EPR measurements [20], allow us to determine the values and the relative signs of the

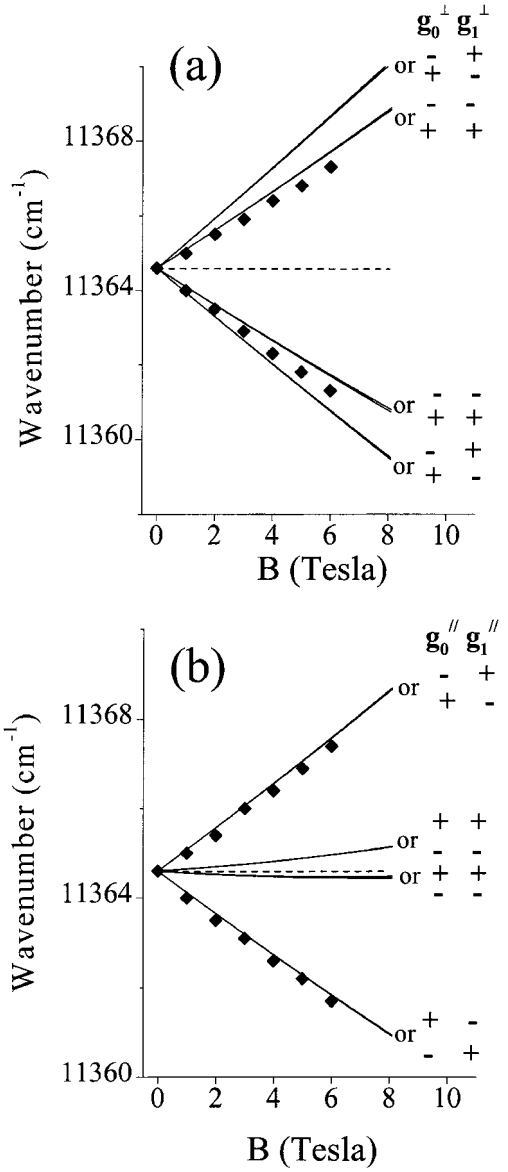

Figure 6. Experimental results (♦) and crystal field simulations of the Zeeman effect on the $^4F_{3/2}(1) \rightarrow {}^4I_{9/2}(1)$ fluorescence transition of isolated Nd^{3+} ions with (a) π-polarization, $B \perp c$, and (b) σ-polarization, $B \parallel c$. All the possible sign combinations of g-values are shown by solid curves.

g-parameters for the three KDs under study. As mentioned in section 3 (see also equation (5)), the observed linear Zeeman splittings of the two $^4F_{3/2}(1$ and $2) \rightarrow {}^4I_{9/2}(1)$ transitions, given in table 1, are $\beta[g_0(\theta) - g_1(\theta)]$. Knowing the absolute values $|g_0|$ of the g-factors of the ground state KD from EPR measurements [20], the g-parameters $|g_1|$ for the $^4F_{3/2}$ KDs could be determined. These g-values are listed in table 2 and are found to be in relatively good agreement with those obtained from crystal field calculations.

Figures 6 and 7 compare the experimental magnetic splitting with the crystal field simulations with all possible sign combinations of the g-factors. The best agreement is obtained for $g_0^\perp$ and $g_1^\perp$ with the same sign and for $g_0^\parallel$ and $g_1^\parallel$ with different signs for the transition $^4F_{3/2}(1) \rightarrow {}^4I_{9/2}(1)$ (figure 6). In contrast, the best agreement between experimental and

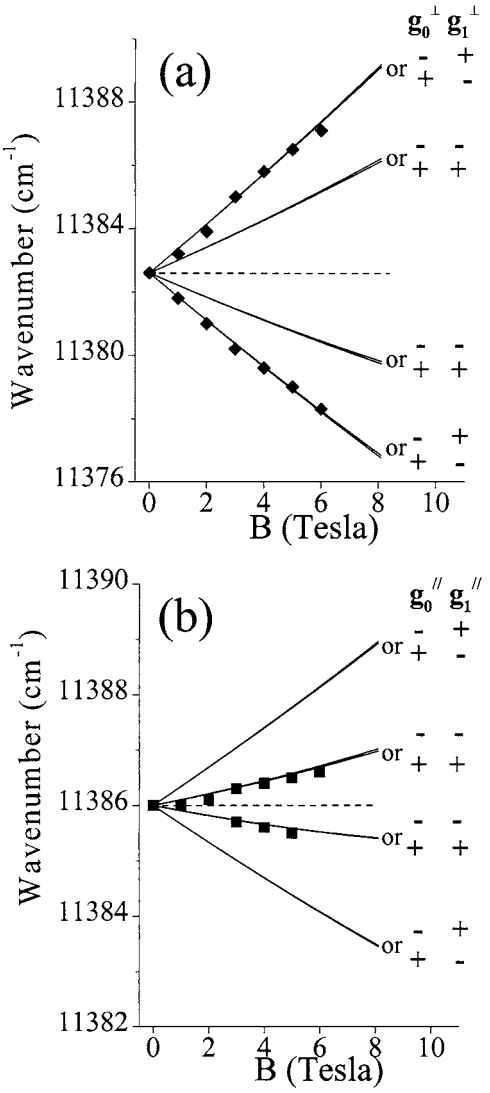

Figure 7. Crystal field simulations of the Zeeman effect on the $^4F_{3/2}(2) \rightarrow {}^4I_{9/2}(1)$ fluorescence transition and the experimental results (a) for isolated Nd^{3+} ions (♦) with π-polarization, $B \perp c$, and (b) for one transition line assigned to the J_4 pair (■) with σ-polarization, $B \parallel c$. All the possible sign combinations of g-values are shown by solid curves.

calculated g-values for the $^4F_{3/2}(2) \rightarrow {}^4I_{9/2}(1)$ transition is obtained for $g_0^{\perp}$ and $g_1^{\perp}$ with different signs and for $g_0^{\parallel}$ and $g_1^{\parallel}$ with same signs (figure 7). Thus, the Zeeman splittings are very sensitive to the relative signs of the g-factors of the electronic states connected by the optical transitions.

5. Conclusion

The multisite character of Nd^{3+} ions in the YVO_4 matrix is investigated by performing Zeeman effect measurements in the high resolution fluorescence spectra. Recently, we have shown that the concentration dependent satellite structure accompanying $^4F_{3/2} \rightarrow {}^4I_{9/2}$ transitions is due to different types of ferromagnetically coupled pairs of neodymium ions, with apparently no crystal field perturbations. The present optical Zeeman effect study confirms that the Nd^{3+} ions forming such pairs are located in the same crystal field environment of D_{2d} symmetry of

the zircon structure, as the isolated Nd^{3+} ions. The Zeeman splittings of the satellite lines are found to be same as that of the parent transitions and are also in good agreement with those simulated from crystal field with D_{2d} point site symmetry. Combination of Zeeman effect and ground state EPR measurements allow us to determine the g-values and their relative signs for the two KDs of the $^4F_{3/2}$ excited state.

However, the reason for the excess of Nd^{3+} ion pairs with respect to a statistical distribution in a weakly doped YVO_4 crystal is still not clear. The ground state exchange interactions of the pairs are of the order of only few cm^{-1} and there are no evident crystal field effects. Then, what could be the driving force that results in a clustering of ions, even at low doping levels, and not in a statistical distribution?

Acknowledgments

The authors are grateful to Dr P Porcher, Dr E Antic-Fidancev, Dr L Beaury and Dr J Derouet for allowing us to use the crystal field calculation software and also for fruitful discussions. We wish to thank Dr B Ferrand from the LETI-CEA for providing the Nd:YVO_4 crystal used in this work.

References

[1] Prinz G A and Cohen E 1968 *Phys. Rev.* **165** 335
[2] Pelletier-Allard N and Pelletier R 1982 *J. Physique* **43** 403
[3] Fricke W Z 1979 *Z. Phys.* B **33** 255, 261
[4] Lupei V, Lupei A, Tiseamu C, Georgescu S, Stoicescu C and Nanau P M 1995 *Phys. Rev.* B **51** 8
[5] Ermeneux F S, Goutaudier C, Moncorgé R, Cohen-Adad M T, Bettinelli M and Cavalli E 1999 *Opt. Mater.* **13** 193
[6] Buisson R and Vial J C 1981 *J. Physique Lett.* **42** L115
[7] Barthem R B, Buisson R, Vial J C and Harmand H 1986 *J. Lumin.* **34** 295
[8] Guillot-Noël O, Mehta V, Viana B, Gourier D, Boukhris M and Jandl S 2000 *Phys. Rev.* B **61** 15 338
[9] Lupei A, Lupei V and Georgescu S 1992 *J. Phys.: Condens. Matter* **4** L221
Pelletier-Allard N, Pelletier R, Tiseanu C and Lupei A 1994 *J. Lumin.* **62** 61
[10] Hehlen M P, Gudel H U, Shu Q, Rai J and Rand S C 1994 *Phys. Rev. Lett.* **73** 1103
Hehlen M P, Kuditcher A, Rand S C and Luthi S R 1999 *Phys. Rev. Lett.* **82** 3050
Hehlen M P, Gudel H U, Shu Q and Rand S C 1996 *J. Chem. Phys.* **104** 1232
[11] Villermain-Lecolier G, Morlot G, Strimer P, Aubry J P and Hadni A 1972 *Phys. Rev.* B **15** 130
[12] Villermain-Lecolier G, Hadni A, Morlot G, Strimer P and Aubry J P 1976 *Infrared Phys.* **16** 605
[13] Enderle M, Pilawa B, Schlaphof W and Kahle H G 1990 *J. Phys.: Condens. Matter* **2** 4685
[14] Couto dos Santos M A, Beaury L, Derouet J and Porcher P 1997 *J. Alloys Compounds* **250** 336
[15] Couto dos Santos M A, Porcher P, Krupa J C and Gesland J Y 1996 *J. Phys.: Condens. Matter* **8** 4643
[16] Carnall W T, Goodman G L, Rajnak K and Rana R S 1989 *J. Chem. Phys.* **90** 3443
[17] Wybourne B G 1965 *Spectroscopic Properties of Rare Earths* (New York: Wiley)
[18] Guillot-Noël O, Kahn-Harari A, Viana B, Vivien D, Antic-Fidancev E and Porcher P 1998 *J. Phys.: Condens. Matter* **10** 6491
[19] Porcher P 1989 FORTRAN programs REEL and IMAGE for simulations of the d^N and f^N configuration involving real and complex crystal field parameters, as well as magnetic field, unpublished
[20] Guillot-Noël O, Simons D and Gourier D 1999 *J. Phys. Chem. Solids* **60** 555